Egyptian Journal of Anatomy, Jul. 2011; 34(2):41-53

Original Article

Effect of Obesity on the Structure and Myoglobin Distribution Within the Lingual Muscles of the Adult Male Albino Rats with Reference to Obstructive Sleep Apnea Syndrome

Nagwa E. El-Nefiawy, Dalia Fawzi Kallini , Azza Kamal Abu-Hussien and Haidy Farid Abdel Hamid

Department of Anatomy, Faculty of Medicine, Ain Shams University.

ABSTRACT

Background: Obesity is recognized as a worldwide health problem. Recently, the prevalence of obesity and concern about its impact on public health has grown dramatically. Obstructive Sleep Apnea Syndrome (OSAS) is the most common type of sleep apnea and the most typical individuals with OSAS suffer from obesity. Maintenance of patent upper airway depends on the dilating forces of the lingual muscles especially the genioglossus muscle which is the principal protrudor muscle of the tongue.

Aim of the work: To find out the impact of obesity on the lingual muscles. Structural changes that occur in the tongue musculature in obese adult albino rats were investigated using light and transmission electron microscopy. Moreover, the state of lingual muscles oxygenation was examined through immune-staining of muscular myoglobin distribution.

Materials and Methods: Three month-old Adult male Albino rats 200 gm body weight were used in the study. Animals were purchased from the Research Unit and Bilharzial Research Center of Faculty of Medicine, Ain Shams University. Rats were divided into two groups (5animals/group). Group I: Control group: Rats were fed a regular diet (protein: Fat: Carbohydrate= 29:13:58, 343 kcal/ 100 g). Group II: Obesity group: Rats were fed a high-fat diet (protein: Fat: Carbohydrate= 20: 57: 23, 508 kcal/ 100 g). After three months, the average weight of the control group was about 312±10 gm, while obesity group was about 730±20 gm. Rats were sacrificed and extracted tongue specimens were processed for light and transmission electron microscopy. Paraffin sections were also immunostained with anti-myoglobin antibody.

Results: Light microscopic examination of lingual muscles of the obese group revealed fatty infiltration, degeneration and necrosis. In addition, congestion of blood vessels and infiltration with mononuclear cellular infiltrate was detected. Transmission electron microscopic investigation showed distortion in the arrangement and destruction of myofibrils and myofilaments. Swelling, apparent increase in number, and distorsion of internal cristae of the mitochondria were observed in obese group tongue muscles versus the control group. Immunohistochemistry for myoglobin revealed weak reaction in obese group compared with the control group.

Conclusion: The present work declared that high-fat diet feeding responsible for rat's obesity induced fat deposition, structural damage, inflammatory cellular infiltration and decreased myoglobin distribution inside lingual myofibres which may interfere with their contractile function. The present results may partially explain the close relationship between obesity and incidence of OSAS.

Key Words: Obesity, tongue, electron microscopy, myoglobin, Obstructive Sleep Apnea Syndrome (OSAS).

Corresponding Author: Dr. Dalia Fawzi Kallini, Anatomy Department, Faculty of Medicine, Ain Shams University, Cairo, Egypt. E-mail: daliakallini@yahoo.com. Mobile: 01221503269.

INTRODUCTION

Obesity is recognized as a worldwide health problem. Overconsumption of fatty foods contributes significantly to this phenomenon. In recent years, the prevalence of obesity and concern about its impact on public health have grown dramatically. Obesity is increasing across all socioeconomic groups and educational levels and occurs even among individuals with the highest level of education *(Gidding et al., 2009)*.

Obstructive Sleep Apnea Syndrome (OSAS) is the most common type of sleep apnea and is caused by obstruction of the upper airway. In adults, the most typical individuals with OSAS

suffer from obesity. OSAS is characterized by repetitive pauses in breathing during sleep and is usually associated with reduction in blood oxygen saturation. These pauses in breathing typically last from 20 to 40 seconds *(Mulgrew et al., 2007; Sutherland et al., 2011; Ye, 2011)*.

Maintenance of the upper airway patent depends on the dilating forces of the lingual muscles such as the genioglosus (GG) and geniohyoid muscles. The genioglossus muscle is considered the principal protrudor muscle of the human tongue. Unlike most skeletal muscles, GG electromyographic activities are robustly preserved during sleep and thus playing critical role in preserving airway patency *(Richardson & Bailey, 2010)*. Moreover, increasing genioglossus muscle activity improves airway patency *(Jordan et al., 2010)*. However, the impact of obesity on the lingual muscles is not fully investigated.

Myoglobin is an iron-and oxygen- binding protein found in muscle tissues of vertebrates. High concentrations of myoglobin in muscle cells allow better muscle function (*Ordway & Garry, 2004*). In case of exercise, the muscles use up any available oxygen. Myoglobin being attached to oxygen provides extra oxygen for the muscle to maintain a high level of activity for a longer period of time. When the muscle is damaged, myoglobin is released into the urine.

The aim of the present study was to investigate the possible structural changes occurring in the tongue musculature of adult male albino rats in case of obesity using light and transmission electron microscopy. Moreover, lingual muscle oxygenation in cases of obesity was investigated through examination of muscular myoglobin distribution using immunohistochemical staining.

MATERIALS AND METHODS

Animals

Three month-old Adult male Albino rats 200 gm body weight were used in the study. Animals were purchased from the Research Unit and Bilharzial Research Center of Faculty of Medicine, Ain Shams University. Rats were maintained under routine conditions with free access to food and water and 12 hours light: 12 hours darkness and were divided into two groups (5 animals/ group),

- **Group I (control group)** rats were fed a regular diet for three month (protein: fat: Carbohydrate= 29: 13: 58, 343 kcal/ 100 g).

- **Group II (obesity group)** rats were fed a high- fat diet for three month (protein: Fat: Carbohydrate= 20: 57: 23, 508 kcal/ 100 g respectively) *(Guillerm-Regost et al., 2006)*.

Rats were weighed regularly every two weeks and also at the end of the experiment to assess their weight. The length of the rat was measured from tip of the nose to the anus to correlate it with the animal's weight to calculate the Body Mass Index (BMI) according to the equation: BMI= Body weight (kg)/length (m^2) according to *(Altunkaynak et al., 2008)*. The average weight of the rats at the start of the experiment was 200 gm. The weight of the control group at the end of the experiment was 312±10 with BMI equal to 5.4±0.2 while that of the obese group was 730±20 with BMI 10.4±0.3.

Body Mass Index (BMI) is a simple index of weight-for-height that is commonly used to classify overweight and obesity in adults as it is the same for both sexes and for all ages. The WHO definition in human is a BMI greater than or equal to 25 is overweight and a BMI greater than or equal to 30 is obesity. While, there is no definition of obesity in laboratory rats. Obesity is usually taken as any significant increase in body weight or energy content relative to control animals *(Novelli et al., 2007)*.

Light microscopic study

After three months of initiating the high-fat diet feeding, all animals were sacrificed with a lethal dose of ether according to the protocol of the Animal Care and Use Commitee of Ain Shams University. Extracted tongue specimens were either divided longitudinally into two equal halves or incised transversely at the posterior 1/3 of the oral part of the tongue. Specimens were fixed in 10% formalin in water for one week, processed and embedded in paraffin. Paraffin sections (4-5-µm thick) were cut and were stained with Haematoxylin, Eosin and toluidine blue stains *(Bancroft & Gamble, 2002)*. The sections were examined with an Olympus light microscope and photographed. Semithin sections were cut (1-µm thick) using LKB microtome from resin embedded blocks for electron microscopy and were stained with 0.5% toluidine blue in water for light microscopic examination.

Transmission Electron Microscopy (TEM)

A part of the extracted tongue specimens was sliced into several tissue pieces with a volume of about 1.0 mm3 for each. These pieces were fixed in 2.5% glutaraldhyde at 4 °C for 2 hrs. After wash with phosphate buffer pH 7.4, they were post-fixed in 1% osmium tetroxide OsO4 at 4 °C for 2 hrs, dehydrated in a graded series of ethanols (50%, 70%, 90%) and embedded in epoxy resin. Ultrathin sections were cut with diamond knives on an ultratome. Sections were stained with uranyl acetate & lead citrate followed by carbon coating. Under transmission electron microscope (TEM-100 SEO), ultrathin sections were observed and photographed *(Graham & Orenstein, 2007)*.

Immuno-histochemical staining for myoglobin

Rabbit polyclonal antibody (ab77232) to myoglobin with species reactivity to skeletal muscles of rat and human was obtained from Abcam (biotech company, UK) and was used at dilution 1:200

Tongue sections were de-paraffinised in xylene, and placed in absolute ethanol. Endogenous peroxidase activity was blocked with 0.3% H_2O_2 in methanol for 20 minutes. To minimize non-specific reaction, sections were initially incubated with fetal calf serum1.5 for 30 min. at 37^0C. Sections were then incubated with anti- myoglobin antibody (Cappel laboratories, USA, 1:200) overnight at 4^oC and rinsed in Phosphate Buffer Saline (PBS). The secondary antibody was then applied to the slides for 30 min. at 37^0C. After another rinse in PBS, sections were incubated with rabbit PAP reagent for 30 min. at 37^0C. Finally sections were treated with diaminobenzidine- H_2O_2 mixture and counterstained with hematoxylin. Negative control staining was performed after omitting the primary antibody *(Bratthauer, 2010)*.

RESULTS

I. Light microscopy

Control group

Each muscle bundle was surrounded by fatty connective tissue sheath, the perimysium. From the perimysium partitions of loose connective tissue (the endomysium) penetrate into each bundle separating the individual muscle fibers (Fig. 1). Individual muscle bundle consisted of thousands of muscle fibres (myocytes) which revealed dotted appearance (Fig. 2). The core of the tongue was formed of bundles of skeletal muscle fibres that were cut in different planes (longitudinal, transverse and vertical) with no branching of the fibres. Nuclei of the cross-sectioned muscle fibres were seen located at the periphery of the muscle fibres immediately under the plasma membrane (sarcolemma). In fibers sectioned longitudinally nuclei occupied any position with respect to fiber breadth (Fig. 3). Fat cells were infrequently observed in the connective tissue between the muscle fibres. Fat cells were recognized by cytoplasmic rims enclosing open spaces that were occupied by the lipid droplets. Oval nuclei of adipocytes were pushed to one side of the cell (Fig. 4).

Obese group

Hx&E and Toluidine blue stained tongue sections of the obesity group revealed apparent relative reduction in the muscle mass. Bundles of lingual muscles appeared compressed away from their connective tissue sheath leaving wide spaces around them compared with the control group (Fig. 5). Many clusters of fat cells were observed in between muscle bundles (Fig. 6) and were particularly localized in close relationship to blood vessels (Fig. 7). Fat cells were characterized by the peripheral localization of their nuclei. In H&E sections the cytoplasm of fat cells revealed empty spaces due to dissolved fat during preparation while fat was preserved and noted in toluidine blue stained sections (Fig. 8). Distorted alignment and ragged myofibres inside muscle bundles could be noticed (Fig. 9). Wide spacing was seen between individual myofibres of lingual muscles (Fig. 9). Pale staining of large scattered patches of the lingual muscles denoting degeneration and necrosis was observed (Fig. 10). Dilatation and congestion of the blood vessels was seen (Fig. 11). Mononuclear cell infiltration was noted within the connective tissue especially in the peri-vascular areas (Figs. 10, 11).

II. Transmission Electron Microscopy

Control group

Examination of the ultrathin sections of the control group revealed the ultrastructure of the

myofibrils which are the structural units of the muscle fibres. The myofibres were bounded by plasma membrane called the sarcolemma (Fig. 12). The nuclei were seen located just beneath the sarcolemma (Fig. 13). Individual myofibres were separated by connective tissue endomysium (Fig. 14). Longitudinally sectioned myofibrils were regularly arranged and revealed numerous myofilaments which had specific, precise and ordered arrangement. A pattern of alternating light and dark bands was seen (Fig. 15). The dark staining band (A-band) was bisected by a thin and light H-band. Thinner band called the M-band bisects the H-band at the middle of the A-band. The adjacent light staining band (I-band) was also bisected by a thin dark line termed the Z-line. The distance between the two Z-lines constituted a unit of skeletal muscle organization known as the sarcomere (Fig. 15). A myofibril consisted of many sarcomeres arranged end to end and each one was of uniform thickness throughout its length. Myofilaments were formed of thick myosin filaments and thin actin filaments (Fig. 16). The myosin myofilaments formed the A-band and the M-band represented the cross bridges that held the myofilaments together, while the actin myofilaments formed the I-band. Mitochondria with their apparent cristae were observed (Fig. 16).

Obese group

Tongue ultrathin sections of the obese rats revealed loss of the normal alignment and distorted arrangement of the myofilaments and the characteristic Z line was hardly seen (Fig. 17). Great variation in the size and shape of the myofilaments were recognized (Fig. 17). Myofilaments lost their precise arrangement and some of them delineated evident signs of degeneration and necrosis (Fig. 18). In some myofibrils nuclear affection was seen in the form of condensation of the nuclear material (pyknosis) (Fig. 19). The sarcoplasm of the myofibrils revealed excessive number of mitochondria in between the myofilaments (Fig. 20). Mitochondria showed marked size variation and sometimes swelling. The outer membrane and inner cristae were intact but some cristae were apparently distorted (Figs. 21, 22).

III. Myoglobin immunohistochemical staining

Examination of the immune-stained sections of the control group revealed dark positive brown reaction localized at the cytoplasm of the myocytes all through the tongue sections and also at the lining of the blood vessels. Sections of the obese group showed weak positive immune staining for myoglobin compared with the control group and revealed the same localization pattern (Figs. 23-26).

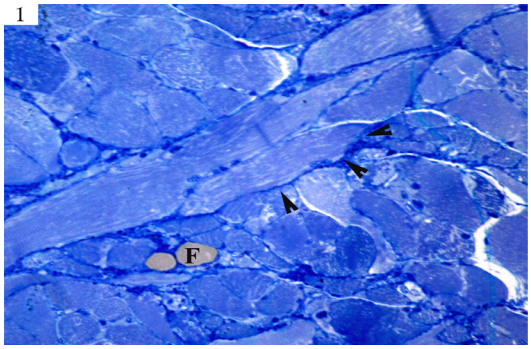

Fig. 1: A photomicrograph of control tongue semithin section of adult male albino rat. Notice the bundle of muscle is enclosed within connective tissue sheath (the perimysium) marked by arrow heads. Notice the fat cell (F). Toluidine blue; x 400

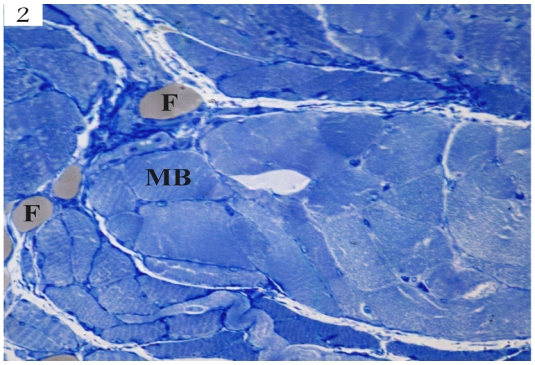

Fig. 2: A photomicrograph of control tongue semithin section of adult male albino rat. Many muscle bundles (MB) are seen that enclose inside thousands of myofibres (muscle fibres) that reveale the dotted appearance. Fat cells (F) can also be seen. Toluidine blue; x 400

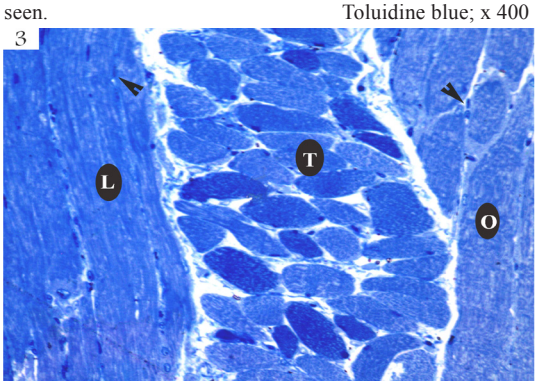

Fig. 3: A photomicrograph of control tongue semithin section of adult male albino rat showing skeletal muscle fibers cut in different directions. Note the presence of longitudinal (L) transverse (T) and oblique (O) bundles of muscles. Muscle fibers nuclei (arrow head) can be seen situated peripherally. Toluidine blue; x 400

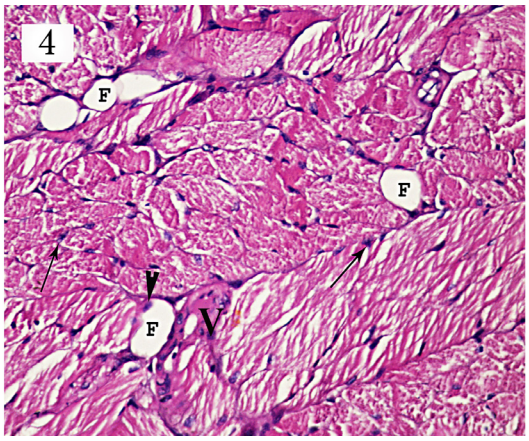

Fig. 4: A photomicrograph of control tongue section of adult male albino rat showing some fat cells (F) with scanty rim of cytoplasm enclosing open spaces and nuclei pushed to one side (arrow head). Notice the peripheral location of muscle fibres nuclei (arrow). Notice the blood vessels (V). Hx. & E.; x 400

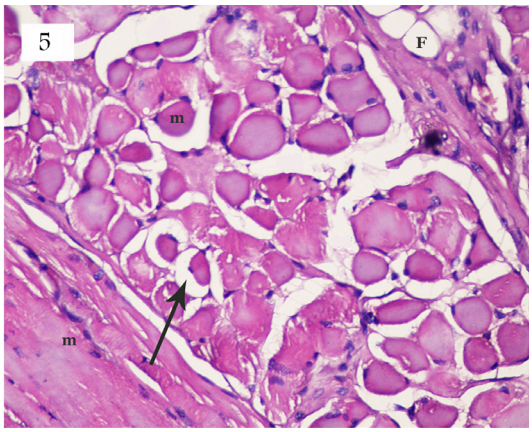

Fig. 5: A photomicrograph of obese tongue section of adult male albino rat showing compressed lingual muscle bundles (m) away from the connective tissue sheath leaving wide spaces (arrow). Fat cells (F) are also seen. Hx. & E.; x 400

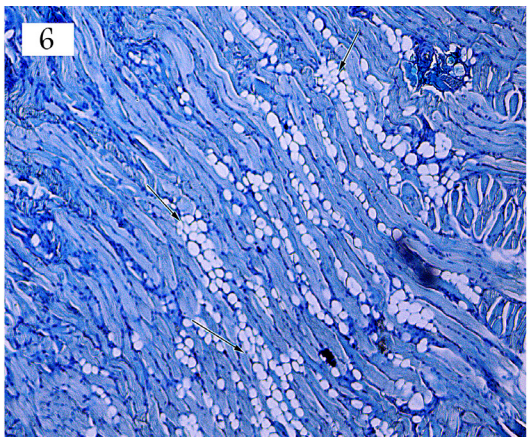

Fig. 6: A photomicrograph of obese tongue section of adult male albino rat showing many clusters of fat cells (arrow) situated among lingual muscle bundles. Toluidine blue; x 100

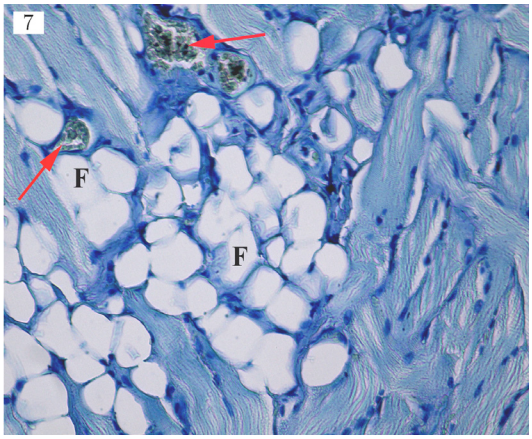

Fig. 7: A photomicrograph of obese tongue section of adult male albino rat showing many clusters of fat cells (F) in the vicinity of the blood vessels (red arrow). Notice the evident wide spacing between myofibres. Toluidine blue; 400

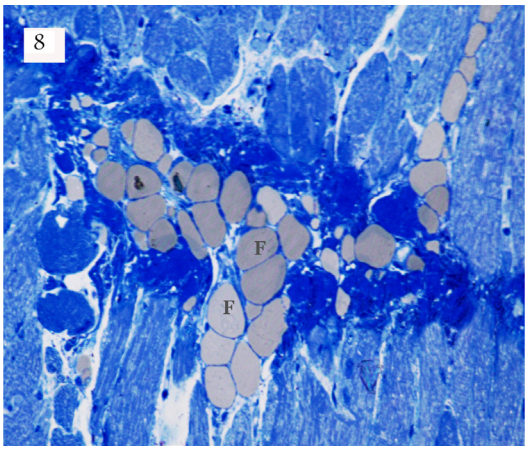

Fig. 8: A photomicrograph of obese tongue semithin section of adult male albino rat showing many fat cells (F) with preserved fat content. Toluidine blue; x 400

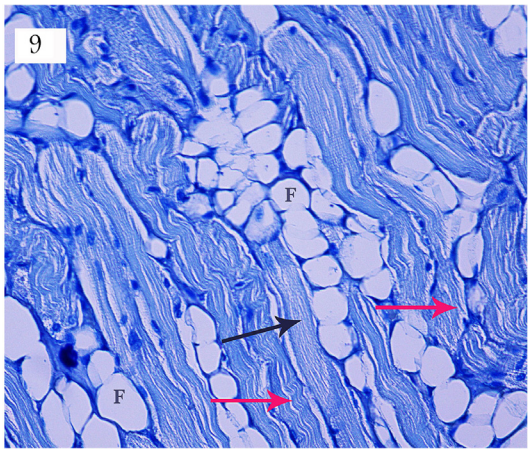

Fig. 9: A photomicrograph of obese tongue section of adult male albino rat showing many fat cells (F) located between muscle bundles. Muscle fibres appear distorted and ragged (red arrow) while few fibres are straight (black arrow). Notice the wide spacing between myofibres inside the bundles. Toluidine blue; x400

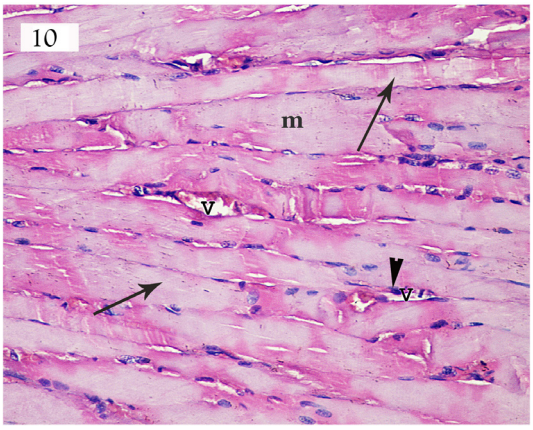

Fig. 10: A photomicrograph of a section of the tongue of an obese adult male albino rat showing multiple scattered patches of pale staining areas (arrow) of the muscle fibres (m) with partial loss of striations. Congested blood vessels (V) are seen. Also note the extensive mononuclear cell infiltrate (arrow head). Hx.& E.; x 400

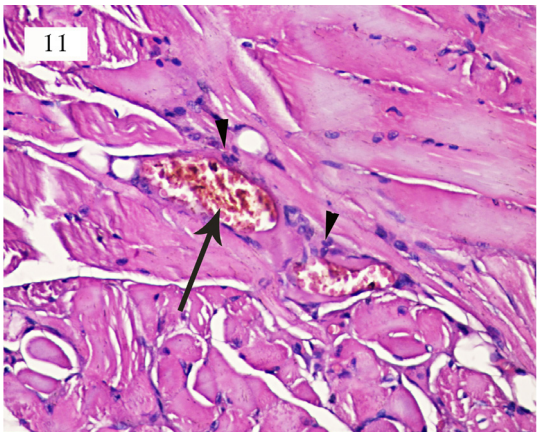

Fig. 11: A photomicrograph of a section of the tongue of an obese adult male albino rat showing congested blood vessels (arrow) surrounded by mononuclear cellular infiltrate particularly in the perivascular area (arrow head). Hx. & E.; x 400

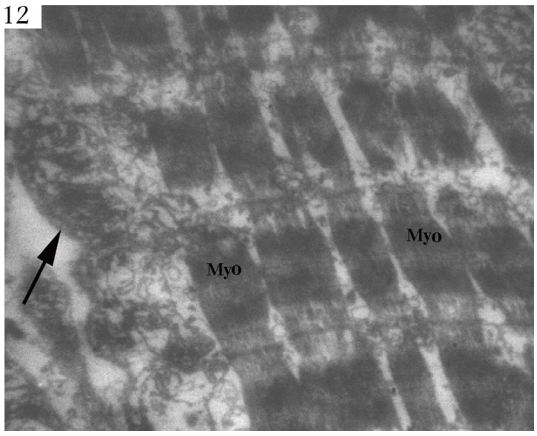

Fig. 12: An electron micrograph of the lingual muscle of control adult male albino rat. Notice the uniform arrangment of myofilaments (Myo) inside a myofibre which is limited by sarcolemma (arrow). Uranyl acetate and lead citrate; x 4,000

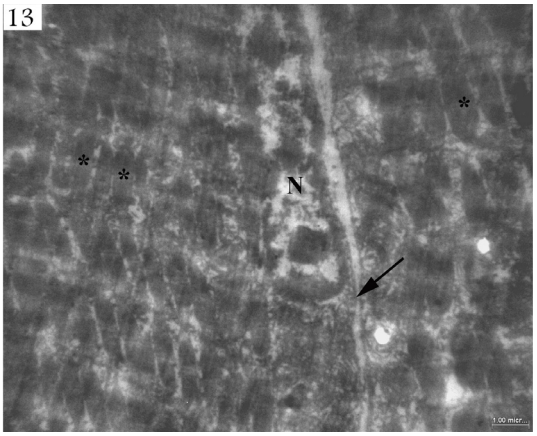

Fig. 13: An electron micrograph of the lingual muscle of control adult male albino rat showing two adjacent myofibres revealing regularly alligned myofilaments (*). The nucleus (N) of myofibre lies under the sarcolemma (arrow). Uranyl acetate and lead citrate; × 4,000

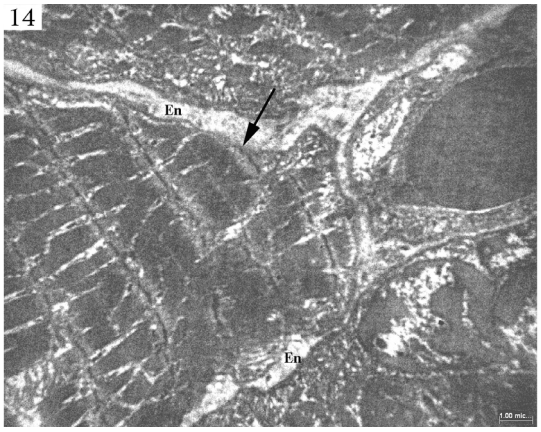

Fig. 14: An electron micrograph of the lingual muscle of control adult male albino rat showing a myofibre surrounded by sarcolemma membrane (arrow). Also connective tissue endomysium (En) separate adjacent myofibres. Uranyl acetate and lead citrate; × 4,000

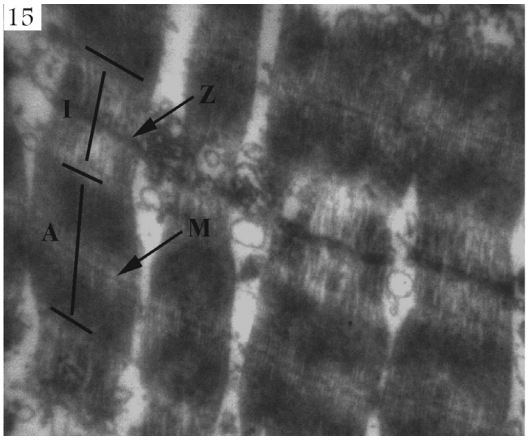

Fig. 15: An electron micrograph of the lingual muscle of control adult male albino rat showing the alternating dark (A) and light bands (I) of the myofilaments. The thin M band bisects the A band and Z line bisects the light band. Uranyl acetate and lead citrate; x 10,000

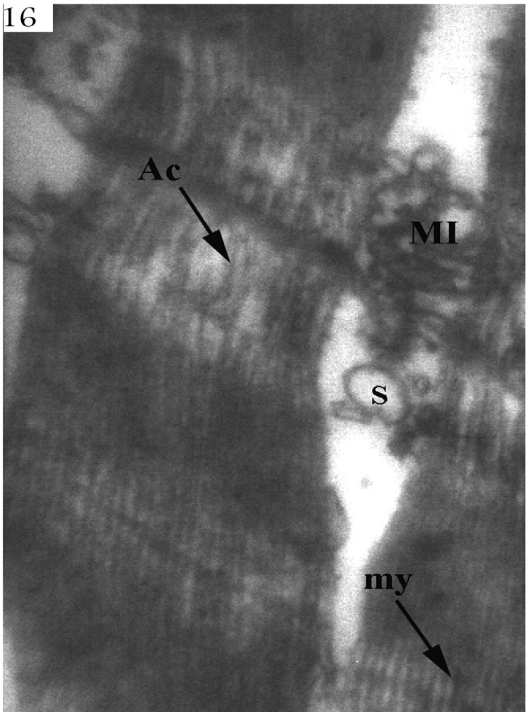

Fig. 16: An electron micrograph of the lingual muscle of control adult male albino rat. Thin actin (AC) in the light band and thick myosin (my) in the dark staining band of the myofilaments can be seen. Mitochondria (MI), and cut sections of the membranes of sarcoplasmic reticulum (S) are also detected inside the sarcoplasm. Uranyl acetate and lead citrate; x 20,000

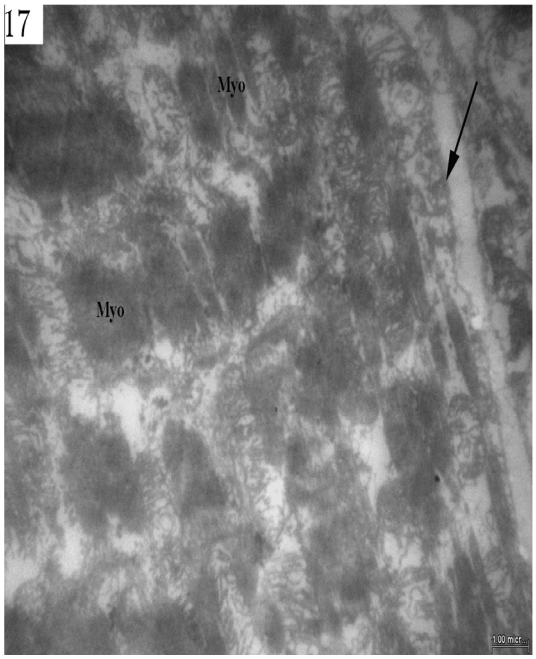

Fig. 17: An electron micrograph of the lingual muscle of obese adult male albino rat. A myofibre can be seen that demonstrates loss of the normal alignment and distorted arrangement of the myofilaments (Myo) inside. Also Z line is nearly lost. Arrow points at sarcolemma membrane. Uranyl acetate and lead citrate; x 4,000

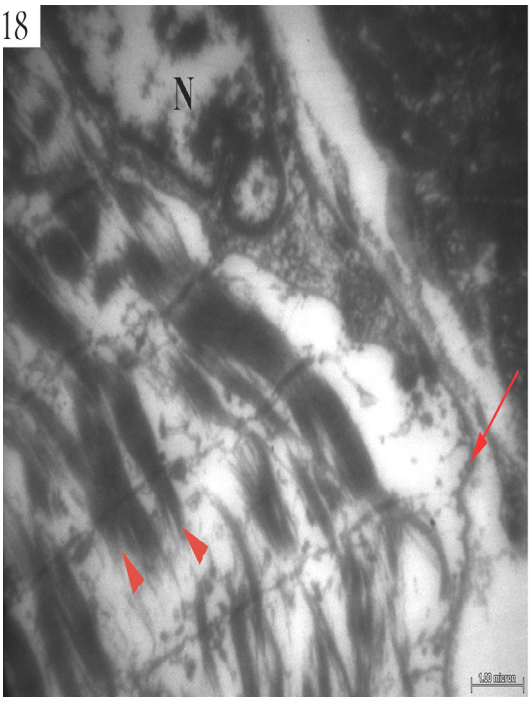

Fig. 18: An electron micrograph of the lingual muscle of obese adult male albino rat. Note myofibre with it's sarcolemma membrane (red arrow) and nucleus (N) underneath. Extensive degeneration and destruction of myofilaments can be seen (red arrow head). Uranyl acetate and lead citrate; x 6,000

Fig. 19: An electron micrograph of the lingual muscle of obese adult male albino rat showing indentation of nuclear membrane (red arrow) and clumping of nuclear chromatin of the nucleus (N). Notice also the excessive mitochondrial numbers (red arrow head) inside the sarcoplasm. Uranyl acetate and lead citrate; x 3,000

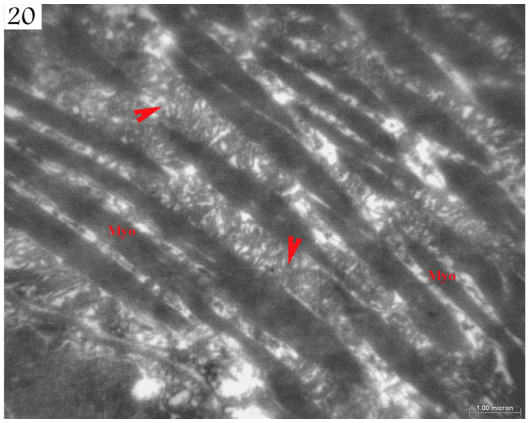

Fig. 20: An electron micrograph of the lingual muscle of obese adult male albino rat showing excessive number of mitochondria (red arrow head) in the sarcoplasm. Mitochondria reveal evident internal cristae. Myofilaments (Myo) reveal distorted regular allignment and inequality in their sizes. Uranyl acetate and lead citrate; x 6,000

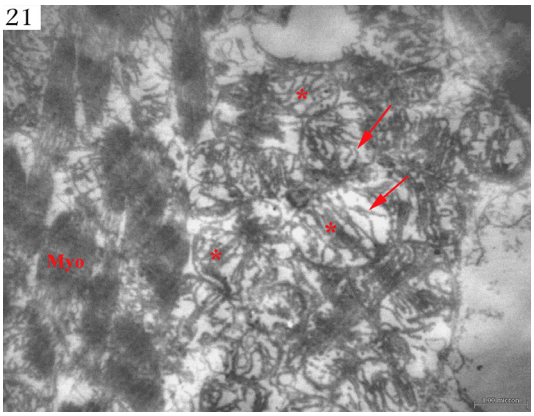

Fig. 21: An electron micrograph of the lingual muscle of obese adult male albino rat. Sarcoplasm of a myofibre demonstrating irregular myofilaments (Myo) and mitochondria (*) with variable sizes with apparent swelling. Some membranes of internal cristae (red arrow) appear distorted. Uranyl acetate and lead citrate; x 6,000

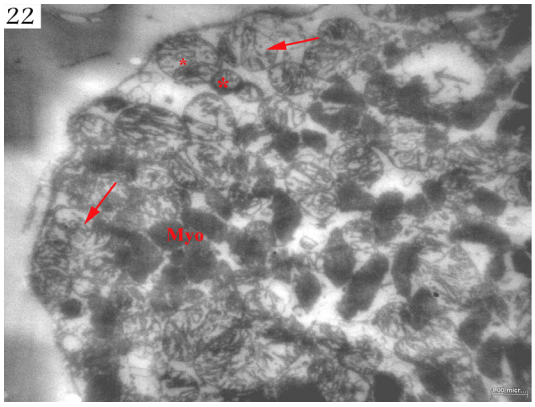

Fig. 22: An electron micrograph of the lingual muscle of obese adult male albino rat showing numerous mitochondria (*) of evident variable sizes and destroyed internal cristae (red arrow). Cut sections of myofilaments (Myo) demonstrate marked irregualrity in size. Uranyl acetate and lead citrate; x 4,000

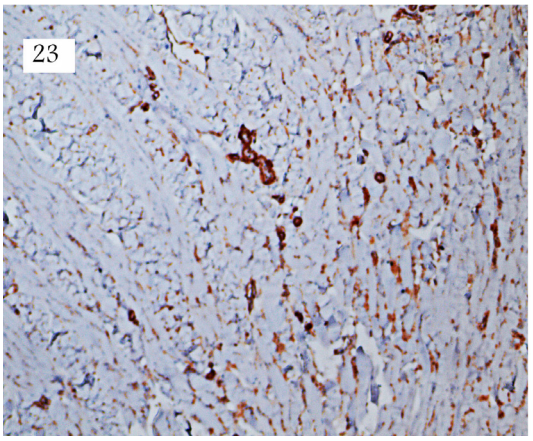

Fig. 23: Photograph of control lingual muscle of adult male albino rat demonstrating strong positive immunostaining (brown colour) for myoglobin localized at sarcoplasm of myofibres. Anti-myoglobin antibody; x 100

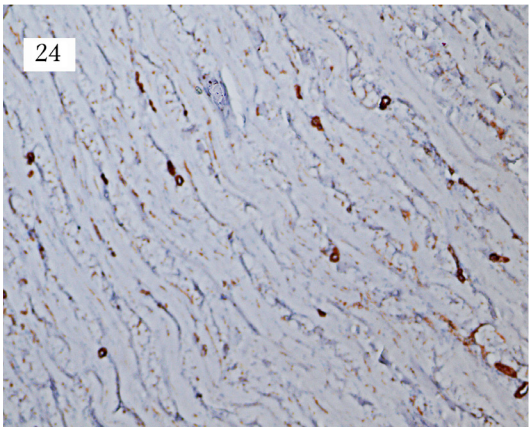

Fig. 24: Photograph of obese lingual muscle of adult male albino rat showing weak positive immunostaining (brown colour) for myoglobin localized at sarcoplasm of myofibres. Anti-myoglobin antibody; x 100

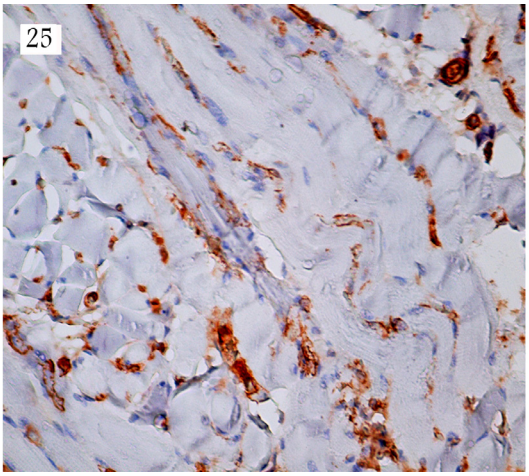

Fig.25: Photograph of control lingual muscle of adult male albino rat showing strong positive immunostaining (brown colour) for myoglobin. Notice the peripheral localization of the positive staining that corresponds to the sarcoplasm of the myofibres. Anti-myoglobin antibody; x 400

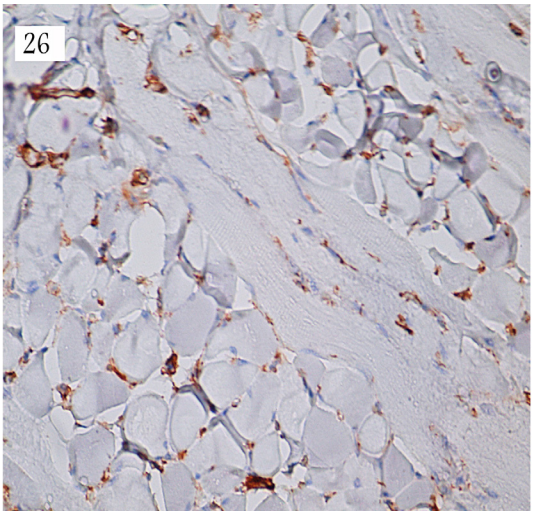

Fig. 26: Photograph of obese lingual muscle of adult male albino rat showing weak positive immunostaining (brown colour) for myoglobin localized at sarcoplasm of myofibres. Anti--myoglobin antibody; x 400

DISCUSSION

The present work investigated the effect of obesity on the structure of the tongue musculature using light and electron microscopic techniques. Also, myoglobin distribution was studied being an essential oxygen-storage hemoprotein capable of facilitating oxygen transport of the muscle.

To investigate why obese patients may have dysfunction of the upper airway dilator muscles, the obese rat model was set up to observe the effects of obesity on lingual muscles. One of the major metabolic anomalies that have been identified in obesity is lipid accumulation in skeletal muscles. In the present work, high fat-diet feeding resulted in fat infiltration in the lingual muscles of the rat with resultant structural changes in the myofibers. Fat cell clusters were seen in large numbers between muscle bundles in the obese group. This is in accordance with *Kelly and Goodpaster (2001), Saito et al. (2010) and Clark et al. (2011).*

Guillerm-Regost et al. (2006) also detected an increase in skeletal muscle lipid content both intra-myocellular within myofiber cytoplasm and extra-myocellular interlaced between muscle fibers in minipigs overfed a hyper-energetic diet during the growth period. The authors explained their findings by decreased lipolysis and fatty acid oxidation. These steps were identified also in the etiology of human obesity. These early metabolic modifications might then precede the enlargement of extra-myocellular and intra-myocellular lipid stores. *Moreover, Corpeleijn, et al. (2008)* stated that obesity is strongly related to disturbances in skeletal muscle lipid metabolism.

The accumulation *of adipose tissue according to Wang et al. (2010)* is the result of increased fat cell size, as well as a result of increased number of fat cells arising from differentiation of pre-adipocytes into mature adipocytes. However, *Clark et al. (2011)* reported an increase in the number of intra-myocellular lipid droplets without large changes in the size of the droplets. In the present study, muscle accretion of fat seemed to arise from an imbalance between lipid deposition and rate of use that led to disturbance in skeletal muscle lipid metabolism.

In the present work, structural changes of the lingual skeletal muscle was observed in the form of multiple patches of pale areas of degeneration with partial loss of striations and regular arrangement of the myofibrils. These changes were also verified by transmission electron microscope. This is in accordance with *Warmington et al. (2000)* who reported reduced ability to undergo hypertrophy in genetically obese mice. The reason suggested for the decrease in muscle mass in these mice was muscle atrophy and not reduction in the total number of muscle fibres present. *Clark et al. (2011)* found an increase in the cross-sectional areas of muscle fibers associated with decrease in slow myosin heavy chains mRNA and protein expression in obese Ossabaw swine. The authors also correlated their findings with those previously reported for obese humans. *Saito et al. (2010)* reported fat deposition in the myofibres of the genioglossus and geniohyoid due to high-fat diet feeding influencing their structure. The diameters of the slow myofibres were approximately 20% greater in the obesity group than in the control group. The percentage of slow fibres to total fibres in the lingual muscles was about 50%. *Guo and Jensen (2003) and Coen et al. (2010)* stated that fat droplets have been found to selectively accumulate in the slow-type fibres of skeletal muscles.

On the contrary, *Carrera et al. (2004)* found that obesity did not influence the structure or function of the genioglosus (GG) by itself. Obesity in the absence of obstructive sleep apnea syndrome (OSAS) does not impose a higher work load upon

the GG. In contrast, in obese patients with OSAS the narrowing of the upper airway may be related more to the deposition of fat tissue around the neck than to mechanical impairment of their upper airway dilator muscles. The authors found that the abnormal fibre-type distribution of the GG was independent of the presence of obesity, indicating that, somehow, this abnormal distribution is a characteristic of the disease itself

Adipocytes help to maintain the appropriate balance between energy storage and expenditure through normal mitochondrial function. Mitochondria play a central role in energy homeostasis through adenosine triphosphate (ATP) production, energy expenditure and disposal of reactive oxygen species *(Bournat & Brown, 2010)*. Defective mitochondrial energy production is implicated in the development and progression of obesity *(Rogge, 2009)*. In the present work, transmission electron microscopy showed that some of the mitochondria appeared distorted with variable shape, size and inapparent cristae. This is in accordance with *Kelley et al. (2002)* who found that the mitochondria of the obese persons revealed less clearly defined inner membrane structures. In addition, *Rogge (2009)* stated that intracellular lipid accumulation contributes to structural abnormalities in the mitochondria. Dysfunctional mitochondria may create a vicious cycle of impaired oxidation. The failure of the skeletal muscle mitochondria to oxidize fat properly leads to increased triglyceride synthesis and ectopic lipid deposits. Cellular infiltration by excess triglycerides impair cellular function, such as muscle contractions and leads to oxidative stress through increased byproducts of lipid peroxidation, increased nitric oxide synthase and inflammatory cytokine production and excess reactive oxygen species formation. These products may damage mitochondrial membranes and DNA, thus jeopardizing mitochondrial respiratory capacity.

The study of *Sebe et al. (1989)* declared that myoglobin immune staining in normal skeletal muscle cells was localized to intracellular cytoplasmic structures like the mitochondria, sarcoplasmic reticulum, the I band and Z line. The authors also indicated that myoglobin localization in muscle cells diminished depending on the grades of muscle cell degeneration as in dystrophic muscle myoglobin fluxes from the muscle cells to extracellular spaces. Y*amashita et al. (2009)* provided evidence that the expression of myoglobin was associated with increased lipid metabolism in muscle and hence decreased amount of lipids. In the present work, immune-staining for myoglobin revealed weak reaction in the obese lingual muscle in contrast to the control group that showed dense immunostaining. Lingual muscle fibres of the obese group were infiltrated by fatty tissue with apparent reduction of the muscle mass and revealed wide patches of degeneration and damage that could explain the weak immunostaining for myoglobin compared with the control group. The present results are in line with previous investigations.

In the present study, salient congestion of the blood vessels and mononuclear inflammatory cellular infiltration were detected in lingual sections of the obese group in contrast to the control group. The present results are in accordance with *Gustafson (2010)* who stated that enlargement of adipocytes, due to impaired adipocyte differentiation led to a chronic state of inflammation in the adipocytes and adipose tissue. This was accompanied with a reduction in the secretion of adiponectin and increase in the secretion of proinflammatory cytokines. *Hirosumi et al. (2002)* found increased activity of serine/threonine kinases, key regulators of inflammation in liver muscle and adipose tissue in cases of obesity. The role of macrophages was also discussed by *Ferrante (2007)* who stated that obesity increases the numbers and activation state of macrophages in adipose tissue thereby contributing significantly to obesity-induced adipose tissue inflammation. *Nishimura et al. (2009)* found that obese adipose tissue of mice fed a high-fat diet contains greater number of activated CD8+effector T cells than CD4+helper T cells infiltration. CD8+T cells result in the accumulation of macrophages.

REFERENCES

Altunkaynak, M. E., Özbek, E., Altunkaynak, B. Z., et al. 2008. The effects of high-fat diet on the renal structure and morphometric parametric of kidneys in rats. Journal of Anatomy 212 (6): 845-852.

Bancroft, J. D. and Gamble, M. 2002. Marsland, Glees and Erikson's techniques: in theory and practice of histological techniques. edited by J. D. Bancroft and M. Gamble, Churchill Livingstone, London, 125.

Bournat, J. C. and Brown, C. W. 2010. Mitochondrial dysfunction in obesity. Current Opinion in Endocrinology, Diabetes and Obesity 17 (5): 446-452.

Bratthauer, G. L. 2010. Overview of antigen detection through enzymatic activity. Methods in Molecular Biology (Clifton, N.J.) 588:231-241.

Carrera, M., Barbe, F., Sauleda, J., et al. 2004. Effects of obesity upon genioglossus structure and function in obstructive sleep apnoea. The European Respiratory Journal: Official Journal of the European Society for Clinical Respiratory Physiology 23 (3):425-429.

Clark, B. A., Alloosh, M., Wenze, J. W., et al. 2011. Effect of diet-induced obesity and metabolic syndrome on skeletal muscles of Ossabaw miniature swine. American Journal of Physiology - Endocrinology and Metabolism 300 (5): E848-E857.

Coen, P. M., Dubé, J. J., Amati, F., et al. 2010. Insulin resistance is associated with higher intramyocellular triglycerides in type I but not type II myocytes concomitant with higher ceramide content. Diabetes 59 (1): 80-88.

Corpeleijn, E., Mensink, M., Kooi, M. E., et al. 2008. Impaired skeletal muscle substrate oxidation in glucose-intolerant men improves after weight loss. Obesity 16 (5): 1025-1032.

Ferrante Jr., A. W. 2007. Obesity-induced inflammation: A metabolic dialogue in the language of inflammation. Journal of Internal Medicine 262 (4): 408-414.

Gidding, S. S., Lichtenstein, A. H., Faith, M. S., et al. 2009. Implementing American heart association pediatric and adult nutrition guidelines. Circulation 119 (8): 1161-1175.

Graham, L., and Orenstein, J. M. 2007. Processing tissue and cells for transmission electron microscopy in diagnostic pathology and research. Nature Protocols 2 (10): 2439-2450.

Guillerm Regost, C., Louveau, I., Sebert, S. P., et al. 2006. Cellular and biochemical features of skeletal muscle in obese Yucatan minipigs. Obesity (Silver Spring) 14 (10): 1700-1707.

Guo, Z. K. and Jensen, M. D. 2003. Accelerated intramyocellular triglyceride synthesis in skeletal muscle of high-fat-induced obese rats. International Journal of Obesity and Related Metabolic Disorders: Journal of the International Association for the Study of Obesity 27 (9): 1014-1019.

Gustafson, B. 2010. Adipose tissue, inflammation and atherosclerosis. Journal of Atherosclerosis and Thrombosis 17 (4): 332-341.

Hirosumi, J., Tuncman, G., Chang, L., et al. 2002. A central role for JNK in obesity and insulin resistance. Nature 420:333-336.

Jordan, A. S., White, D. P., Owens, R. L., et al. 2010. The effect of increased genioglossus activity and end-expiratory lung volume on pharyngeal collapse. Journal of Applied Physiology 109 (2): 469-475.

Kelley, D. E. and Goodpaster, B. H. 2001. Effects of exercise on glucose homeostasis in Type 2 diabetes mellitus. Medicine and Science in Sports and Exercise 33 (6 Suppl): S495-529.

Kelley, D. E., He, J., Menshikova, E. V. and Ritov, V. B. 2002. Dysfunction of mitochondria in human skeletal muscle in type 2 diabetes. Diabetes 51 (10): 2944-2950.

Krenacs, T., Molnar, E., Dobo, E. and Dux, L. 1989. Fibre typing using sarcoplasmic reticulum Ca2+-ATPase and myoglobin immunohistochemistry in rat gastrocnemius muscle. The Histochemical Journal 21 (3): 145-155.

Mulgrew, A. T., Fox, N., Ayas, N. T. and Ryan, C. F. 2007. Diagnosis and initial management of obstructive sleep apnea without polysomnography: A randomized validation study. Annals of Internal Medicine 146 (3): 157-166.

Nishimura, S., Manabe, I., Nagasaki, M., et al. 2009. CD8+effector T cells contribute to macrophage recruitment and adipose tissue inflammation in obesity. Nature Medicine 15 (8): 914-920.

Novelli, E. L. B., Diniz, Y. S., Galhardi, C. M., et al. 2007. Anthropometrical parameters and markers of obesity in rats. Laboratory Animals 41 (1): 111-119.

Ordway, G. A. and Garry, D. J. 2004. Myoglobin: An essential hemoprotein in striated muscle. Journal of Experimental Biology 207 (20): 3441-3446.

Richardson, P. A. and Fiona Bailey, E. 2010. Tonically discharging genioglossus motor units

show no evidence of rate coding with hypercapnia. Journal of Neurophysiology 103 (3): 1315-1321.

Rogge, M. M. 2009. The role of impaired mitochondrial lipid oxidation in obesity. Biological Research for Nursing 10 (4): 356-373.

Saito, T., Yamane, A., Kaneko, S., et al. 2010. Changes in the lingual muscles of obese rats induced by high-fat diet feeding. Archives of Oral Biology 55 (10): 803-808.

Sebe, T., Kawai, H., Nishida, Y., et al. 1989. Changes in myoglobin localization in the skeletal muscle of neuromuscular diseases demonstrated by immunohistochemistry and immunoelectron microscopy. Rinsho Shinkeigaku. Clinical Neurology 29 (7): 835-843.

Sutherland, K., Deane, S. A., Chan, A. S. L., et al. 2011. Comparative effects of two oral appliances on upper airway structure in obstructive sleep apnea. Sleep 34 (4): 467-477.

Wang, Y., Hudak, C. and Sul, H. S. 2010. Role of preadipocyte factor 1 in adipocyte differentiation. Clinical Lipidology 5 (1): 109-115.

W***armington, S. A., Tolan, R. and McBennett, S. 2000.*** Functional and histological characteristics of skeletal muscle and the effects of leptin in the genetically obese (ob/ob) mouse. Journal of the International Association for the Study of Obesity 24 (8): 1040-1050.

Yamashita, H., Maruta, Y. H., Jozuka, M., et al. 2009. Effects of acetate on lipid metabolism in muscles and adipose tissues of type 2 diabetic otsuka long-evans tokushima fatty (OLETF) rats. Bioscience, Biotechnology and Biochemistry 73 (3): 570-576.

Ye, L. 2011. Factors influencing daytime sleepiness in Chinese patients with obstructive sleep Apnea. Behavioral Sleep Medicine 9 (2): 117-127.

تأثير البدانة علي التركيب البنائي وتوزيع الميوجلوبين فى عضلات اللسان عند ذكور الجرذان البيضاء، مع الاشارة الي متلازمة إنقطاع النفس الإنسدادى عند النوم

نجوى إبراهيم النفياوى، داليا فوزى قلينى، عزه كمال أبو حسين، هايدى فريد عبد الحميد

قسم التشريح – كلية الطب – جامعة عين شمس

ملخص البحث

تعد البدانة من أكثر المشكلات الصحية عالميا والتى تزايدت بشكل ملحوظ فى السنوات الأخيرة. وترتبط متلازمة إنقطاع النفس الإنسدادى عند النوم ارتباطا وثيقا بالبدانة. وتلعب عضلات اللسان دورا رئيسيا فى منع ارتجاع اللسان الى الخلف أثناء النوم والذي يعد من اهم اسباب حدوث هذه المتلازمة.

و قد أ جريت هذه الدراسة لمعرفة التغيرات البنائية فى عضلات اللسان فى ذكور الجرذ الأبيض البالغ البدين وذلك بإستخدام المجهر الضوئى والألكترونى بالإضافة الى فحص الميوجلوبين العضلى للتعرف على كيفية مد عضلات اللسان بالأكسوجين وذلك بإستخدام تقنية الصباغة المناعية.

ولقد إستخدم فى هذه الدراسة ذكور جرذان بيضاء بالغة تبلغ من العمر ثلاثة شهور، و كانت أوزانها حوالي ٢٠٠ جم. وقد قسمت الفئران الى مجموعتين (خمسة جرذان فى كل مجموعة): المجموعة الأولى أستخدمت كمجموعة ضابطة تم اعطاء الفئران فيها وجبات معتادة. والمجموعة الثانيه تم إعطاؤها وجبات عالية الدهون فتزايد وزنها بشكل ملحوظ.

و تم التضحية بالفئران من المجموعتين بعد ثلاثة شهور و تمرير العينات لفحصها بالميكروسكوب الضوئي و الالكتروني النافذ.

و قد أوضحت النتائج أن عضلات لسان الجرذان البدينه أظهرت تحللا فى الأنسجة وأنتشارا للدهون بها وأرتشاح خلوى واحتقان فى الأوعية الدموية وأظهر الميكروسكوب الألكترونى تشوها فى الألياف العضلية وكذلك بالميتوكوندريا.

كما أظهرت التقنيه الهستولوجية الكيميائية المناعية تفاعلا ضعيفا مع الميوجلوبين فى المجموعة التى تعانى من البدانه مقارنه بالمجموعة الضابطة مما يفسر تعرضها لنقص الأكسوجين بالألياف العضلية.

وقد تم إستنتاج أن الغذاء عالى الدهون والذى كان مسئولا عن بدانه الجرذان قد أدى الى ترسب الدهون وإختلال التركيب البنائى ونقص بروتين العضلات بداخل الألياف العضلية فى اللسان، مما قد يفسر ارتباط متلازمة إنقطاع النفس الإنسدادى عند النوم بالبدانة.